JOURNAL OF VIROLOGY, May 1997, p. 3811–3816 Vol. 71, No. 5
0022-538X/97/$04.00+0

Functional Equivalence of Common and Unique Sequences in the 3′ Untranslated Regions of Alfalfa Mosaic Virus RNAs 1, 2, and 3

CLEMENS M. A. VAN ROSSUM, FRANS T. BREDERODE, LYDA NEELEMAN, AND JOHN F. BOL*
Institute of Molecular Plant Sciences, Gorlaeus Laboratories, Leiden University, 2300 RA Leiden, The Netherlands

Received 25 September 1996/Accepted 10 February 1997

The 3′ untranslated regions (UTRs) of alfalfa mosaic virus (AMV) RNAs 1, 2, and 3 consist of a common 3′-terminal sequence of 145 nucleotides (nt) and upstream sequences of 18 to 34 nt that are unique for each RNA. The common sequence can be folded into five stem-loop structures, A to E, despite the occurrence of 22 nt differences between the three RNAs in this region. Exchange of the common sequences or full-length UTRs between the three genomic RNAs did not affect the replication of these RNAs in vivo, indicating that the UTRs are functionally equivalent. Mutations that disturbed base pairing in the stem of hairpin E reduced or abolished RNA replication, whereas compensating mutations restored RNA replication. In vitro, the 3′ UTRs of the three RNAs were recognized with similar efficiencies by the AMV RNA-dependent RNA polymerase (RdRp). A deletion analysis of template RNAs indicated that a 3′-terminal sequence of 127 nt in each of the three AMV RNAs was not sufficient for recognition by the RdRp. Previously, it has been shown that this 127-nt sequence is sufficient for coat protein binding. Apparently, sequences required for recognition of AMV RNAs by the RdRp are longer than sequences required for CP binding.

Alfalfa mosaic virus is classified as the only member of the *Alfamovirus* genus, belonging to the *Bromoviridae*. In our previous papers, alfalfa mosaic virus was abbreviated as AlMV. Following the recommendation of the International Committee on Taxonomy of Viruses, we will use the abbreviation AMV in subsequent papers (15). Members of the *Bromoviridae* family of plant viruses share the property of having a tripartite genome consisting of messenger-sense single-stranded RNA molecules. RNA 1 and RNA 2 of these viruses each encodes a subunit of the viral RNA-dependent RNA polymerase (RdRp). In the case of AMV, these proteins are designated P1 and P2, respectively. RNA 3 can be translated into the putative movement protein (P3 in AMV), and from it a subgenomic mRNA (RNA 4) can be derived that can be translated into the viral coat protein (CP).

The RNAs of a virus belonging to the *Bromoviridae* typically share a homologous region of about 150 to 200 nucleotides (nt) at their 3′ ends. In members of the genera *Bromovirus* and *Cucumovirus*, part of this homologous region can be folded into a tRNA-like structure (TLS). Members of the *Ilarvirus* and *Alfamovirus* genera lack this TLS. Instead, the 3′ homologous regions of these viruses are characterized by the presence of multiple predicted stem-loop structures flanked by AUGC sequence motifs. These elements have been shown to serve as high-affinity binding sites for the CP. The presence of these CP binding sites correlates with a unique feature of AMV and the ilarviruses: the fact that a mixture of the genomic RNAs is not infectious to plants unless CP or its mRNA, RNA 4, is present in the inoculum. This phenomenon has been termed genome activation (1).

The 3′ untranslated regions (UTRs) of AMV RNAs 1 (163 nt), 2 (166 nt), and 3 (179 nt) contain a 3′-terminal homologous region of 145 nt. Despite nucleotide sequence variation at 22 positions in this 145-nt-long region, a nearly identical secondary structure could be proposed for this common region in all AMV RNAs (13) (see Fig. 1). The observation that these nucleotide differences are strictly conserved during serial passage of the virus could suggest that they have a specific effect on replication, translation, or encapsidation of the different AMV RNAs. Alternatively, the common regions could be seen as functionally equivalent variants of the 3′-terminal sequence which cannot be freely exchanged between the different AMV RNA species in nature. To study their functional equivalence, we have exchanged either the complete 3′ UTRs or the homologous regions of the three genomic RNAs. The replication of chimeric RNAs was analyzed in tobacco plants. In addition, a deletion analysis was done to identify 3′-terminal sequences of RNAs 1, 2, and 3 involved in recognition of the RNAs by the solubilized AMV RdRp in an in vitro RNA polymerase essay. The results showed that the 3′ common sequences of 145 nt as well as the full-length UTRs of AMV RNAs 1, 2, and 3 can be exchanged without a detectable effect on RNA replication. Moreover, a mutational analysis underlined the importance for RNA replication of one of the stem-loop structures in the homologous region of 145 nt.

MATERIALS AND METHODS

Construction of mutant AMV cDNA clones. The cDNA clones of AMV RNAs 1, 2, and 3 contain *Dra*III restriction sites 127 bp from their 3′ ends. This site was used to exchange the sequence of the 3′-most 127 nt between infectious cDNA clones of the genomic RNAs flanked by the cauliflower mosaic virus 35S promoter and nopaline synthase terminator (hereafter referred to as 35S/cDNAs) (17). These clones were digested with *Dra*III and *Kpn*I, which cleaves in the vector sequence upstream of the CaMV 35S promoter, and the appropriate fragments were ligated to give mutants 1D2, 1D3, 2D1, 2D3, 3D1, and 3D2 (see Fig. 2). Mutant 1D2 contains the sequence upstream of the *Dra*III site from RNA 1 and the sequence downstream of this site from RNA 2, etc. The wild-type (wt) DNA 1 construct (designated 1 WT [see Fig. 2]) was used as the template in a PCR reaction primed by oligonucleotides 5′ TAACC***CACCCAGTG***GAGG TCAGCATTGAATTACC 3′ (complementary to nt 3492 to 3525 of RNA 1; boldface italics represent the *Dra*III restriction site, and the mutated nucleotides are underlined) and 5′ CCAATATCAAGCAAATAGCCCG 3′ (corresponding to nt 2637 to 2658 of RNA 1). The PCR product was digested with *Nco*I and *Dra*III, and the resulting fragment was inserted in *Nco*I- and *Dra*III-digested

* Corresponding author. Mailing address: Gorlaeus Laboratories, Leiden University, Einsteinweg 55, 2333 CC Leiden, The Netherlands. Phone: 31-71-5274749. Fax: 31-71-5274340. E-mail: J.BOL@chem.LeidenUniv.nl.

plasmids 1WT and 1D3 to produce the constructs 1UG and 1UGD3, respectively (see Fig. 2).

Fusion of the bacteriophage T7 promoter sequence to AMV cDNAs 1 and 2 was accomplished by cDNA synthesis on partially purified RNA 1 or RNA 2. By using reverse transcriptase, single-stranded cDNA was produced, primed by the oligonucleotide 5′ CCTTTGTCTGAAGGGAGAGC 3′ (complementary to nt 269 to 288 of RNA 1). To this cDNA the oligonucleotide 5′ GG*AAGCTT*TAA TACGACTCACTATAGGTTTTTATCTTACA 3′ (which contains a *Hin*dIII restriction site [in boldface italics]) was annealed, after which were added a T7 promoter, an extra G residue, and 14 nt corresponding to the 5′ end of AMV RNA 1 (underlined). Second-strand cDNA was synthesized by using reverse transcriptase. The double-stranded DNA was digested with *Hin*dIII and *Pst*I. The fragment corresponding to the 5′ end of AMV RNA 1 was fused to the remaining cDNA 1 sequence derived from the infectious 35S/cDNA clone and inserted in *Hin*dIII- and *Sma*I-digested pUC 9 plasmid. In a similar way, the AMV cDNA 2 was fused to the T7 promoter (incorporating one extra G residue at the 5′ end of the viral sequence) and cloned into *Hin*dIII- and *Pst*I-digested pUC 9. Deletion mutants of RNAs 1 and 2 (see Fig. 4) were constructed by transferring relevant restriction fragments, encompassing the deletions, from previously engineered deletion mutants in the corresponding 35S/cDNA constructs (35). cDNA 1 deletion mutants are as follows (with the deleted nucleotides in brackets): 1-ΔPS (205 to 357), 1-ΔPAp (205 to 1107), 1-ΔHEn (1118 to 1424), 1-ΔEnBs (1425 to 2059), 1-ΔBsXb (2064 to 2464), and 1-ΔXbD (2469 to 3517). cDNA 2 deletion mutants are 2-ΔNXh (57 to 262), 2-ΔXhEn (266 to 406), 2-ΔEnA (408 to 1105), 2-ΔAEv (1110 to 1488), 2-ΔEvBg (1489 to 2297), and 2-ΔBgD (2302 to 2466).

Transcription plasmids in which the 3′ UTR of RNA 3 was replaced by that of RNA 1 or RNA 2 were constructed from T7-3K (see Fig. 4). In this construct, a *Kpn*I restriction site is located directly downstream of the CP open reading frame (31). Oligonucleotides 5′ CTAC*GGTACC*CATTGGTAATTCAATGCCAACC TCC 3′ and 5′ CTAC*CTGCAG*CATCCCTTAGGGGCATTC 3′ (boldface italics indicate introduced *Kpn*I and *Pst*I restriction sites) were used in a PCR reaction to amplify the sequence corresponding to the 3′ UTR of AMV RNA 1, flanked by *Kpn*I and *Pst*I restriction sites. The PCR product was digested with *Kpn*I and *Pst*I and inserted into the T7-3K plasmid digested with the same enzymes, producing T7-3K1. The plasmid T7-3K2, containing the 3′ UTR from RNA 2, was constructed in the same way, using oligonucleotide 5′ CTAC*GGTACC*CTT GACATAAGTCAAATTGCCAACC 3′ together with the oligonucleotide containing the *Pst*I restriction site. Mutants T7-3ΔKD1, T7-3ΔKD2, and T7-3ΔKD were constructed by digesting plasmids T7-3K1, T7-3K2, and T7-3K, respectively, with *Kpn*I and *Dra*III. Blunt ends were generated by using T4 DNA polymerase, after which the DNA was religated. In these mutants, the 3′-terminal 127 nt of AMV RNA 1, 2, or 3 are placed directly behind the CP open reading frame. Mutants T7-3D1 and T7-3D2 were constructed by inserting the *Dra*III-*Pst*I fragments from T7-3K1 and T7-3K2 in *Dra*III- and *Pst*I-digested T7-3. T7-3D1 and T7-3D2 correspond to mutants 3D1 and 3D2 but contain the T7 promoter instead of the 35S promoter. Mutant T7-3UG was constructed by amplifying a 3′-terminal fragment on AMV cDNA 3, using oligonucleotide 5′ CCTC*CACTG GGTG*GATTAAGTTGAGGTATGAAG 3′ (corresponding to nt 2006 to 3039 of RNA 3; boldface italics represent a *Dra*III restriction site, and mutated nucleotides are underlined) in combination with the oligonucleotide complementary to the 3′ end that contains a *Pst*I site (described above). The PCR product was digested with *Dra*III and *Pst*I and inserted in plasmid T7-3 (wt) digested with the same enzymes. All recombinant DNAs were checked by restriction mapping and sequence analysis.

In vitro transcription. Plasmids containing AMV cDNAs fused to the T7 promoter were linearized with *Sma*I (for cDNA 1) or *Pst*I (for cDNAs 2 and 3). *Pst*I sites were converted to blunt ends by treatment with T4 DNA polymerase. In vitro transcription with T7 RNA polymerase was performed with 2 μg of template DNA in a reaction volume of 100 μl as described previously (29). RNA 1 transcripts carry two nonviral C residues at the 3′ terminus, and the RNA 1 and 2 transcripts have one nonviral G residue at the 5′ terminus. For inoculation of tobacco plants with wt or mutant RNA 3 transcripts, 20 μl of the transcription mixture was used without further treatments. Transcripts were extracted with phenol-chloroform before being used as the template in the RdRp reaction.

Inoculation of plants. Nontransgenic *Nicotiana tabacum* cv. Samsun NN and transgenic P1, P2, and P12 plants were grown and inoculated with 35S/cDNA constructs or RNA 3 transcripts as described previously (17, 26). Each sample was inoculated on two plants, using three half-leaves per plant.

Analysis of viral RNA. Total RNA was extracted from infected leaves as described previously (30) and analyzed by Northern blot hybridization. Random-primed cDNA 3 or a mixture of random-primed cDNAs 1, 2, and 3 was used as a probe (6). The amount of RNA loaded per slot corresponded to 5 mg of leaf material.

RdRp assay. *Nicotiana benthamiana* plants infected with AMV were used to purify the AMV RdRp as described previously (18). Such a preparation is highly specific and is dependent on added AMV template RNAs for its activity. This enzyme was used to study minus-strand RNA synthesis on T7 transcripts of modified AMV cDNA constructs by incorporation of [α-^{32}P]UTP followed by S1 nuclease treatment, electrophoresis of the products on agarose gels, and autoradiography, all essentially as described previously (2, 9).

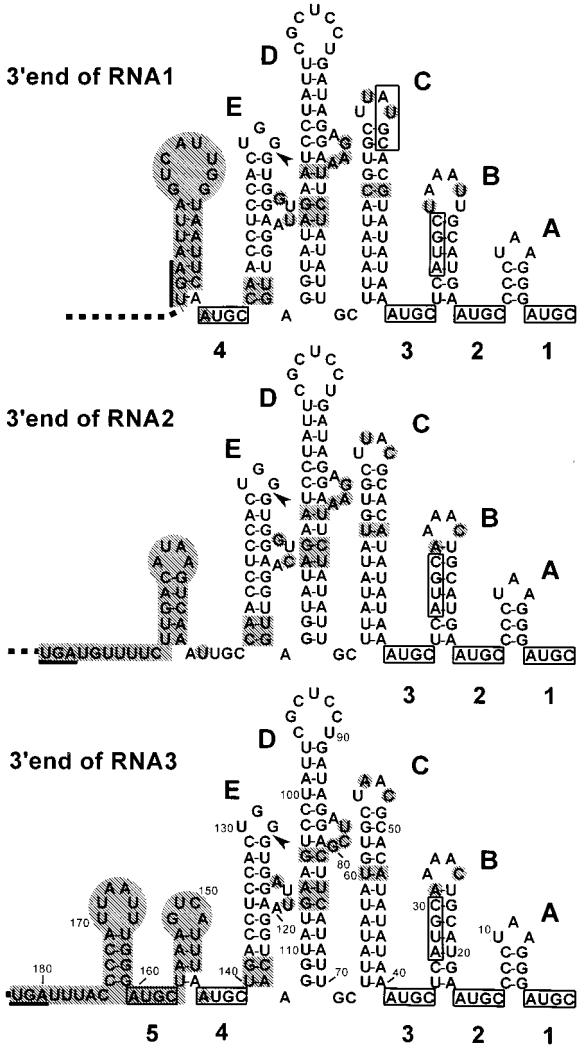

FIG. 1. Schematic representation of the proposed secondary structure of the 3′ UTRs of the genomic RNAs of AMV. The structure prediction for the homologous region is based on the GCG computer program MFOLD. Shading indicates bases which are not identical in all three RNAs. The black bars indicate the stop codons of the P1, P2, and CP open reading frame in RNAs 1, 2, and 3, respectively. AUGC sequence motifs are boxed. The AUGC boxes involved in CP binding in RNA 3 are numbered, as are their counterparts in RNAs 1 and 2. Proposed stem-loop structures are labeled A to E. The arrowheads indicate the positions of unique *Dra*III restriction sites in the viral cDNAs. The nucleotides in the RNA 3 sequence are numbered from the 3′ end.

RESULTS

Exchange of the common regions of the 3′ UTRs. Figure 1 illustrates that the 3′ homologous sequence in the AMV RNAs extends 5 nt upstream of the region containing stem-loop structures A to E. Most of the sequence variations in this common region are located downstream of the *Dra*III restriction site in the cDNA corresponding to the loop of hairpin E. This restriction site was used for exchange of the 127-nt 3′-terminal sequence between the AMV RNAs. Figure 2 shows schematic representations of the putative structure of hairpin E in the mutant RNAs that are expressed from the chimeric AMV 35S/cDNAs. Sequences upstream and downstream of the *Dra*III site (marked D in Fig. 2) corresponding to RNAs 1, 2, and 3 are indicated as 1, 2, and 3, respectively. 35S/cDNAs corresponding to wt RNAs 1, 2, and 3 are designated 1WT, 2WT, and 3WT, respectively, in Fig. 2. The bottom of hairpin

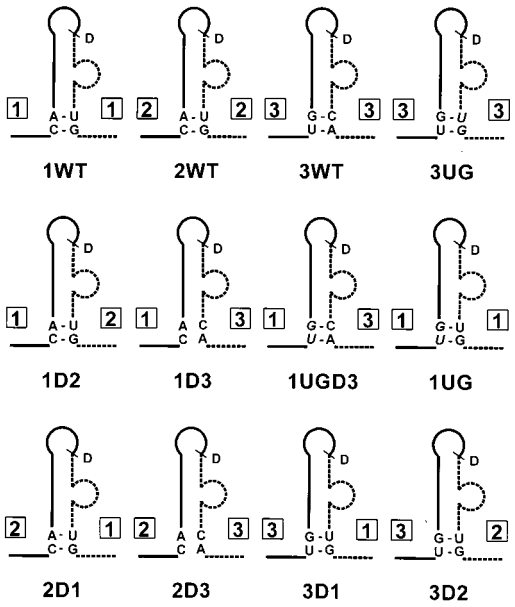

FIG. 2. Schematic representation of stem-loop structure E in wt and mutant AMV RNAs. Only the bases at the bottom of this structure are drawn; the other bases are represented by a line. The letter D indicates the position of the *Dra*III restriction site, which was used to construct the mutants. Boxed numbers indicate the viral RNA from which the sequence 5′ or 3′ to the *Dra*III site was derived. Bases in italics represent modifications achieved by site-directed mutagenesis.

E is closed by A-U and G-C base pairs in RNAs 1 and 2 and by G-C and U-A base pairs in RNA 3. Therefore, exchange of the 3′-terminal 127 nt between RNAs 1 and 2 (mutants 1D2 and 2D1) does not affect the base pairing in hairpin E. However, in mutants 1D3 and 2D3, the two bottom base pairs of hairpin E are replaced by two A-C mismatches, whereas in mutants 3D1 and 3D2, two U-G base pairs are formed.

Tobacco plants were inoculated with a mixture of 35S/cDNAs of the three genomic RNAs with 3′-terminal sequences of 127 nt derived from RNA 1 (1WT, 2D1, and 3D1), RNA 2 (1D2, 2WT, and 3D2), or RNA 3 (1D3, 2D3, and 3WT). 35S/cDNA 4, which enhances infection (17), was omitted in these experiments to avoid the presence of different 3′-terminal sequences in the inoculum. Figure 3 shows the results of a Northern blot analysis of the accumulation of viral RNAs in the inoculated leaves. Accumulation of RNAs with the 3′-terminal sequence of RNA 1 (lane 2) or RNA 2 (lane 3) is similar to accumulation of the wt RNAs (lane 1). However, no RNA accumulation was observed in the plants inoculated with mutants containing the RNA 3-derived 3′-terminal sequence (Fig. 3, lane 4). This lack of biological activity could be due to a defect in mutant 1D3, in mutant 2D3, or in both mutants. To discriminate among these possibilities, transgenic tobacco plants transformed with the P1 gene (P1 plants) or P2 gene (P2 plants) were used. P1 plants support the replication of RNAs 2 and 3 when inoculated with wt 35S/cDNAs 2, 3, and 4 (17) (Fig. 3, lane 5). When the 35S/cDNA 2 in this inoculum was replaced by mutant 2D3, no RNA accumulation was observed (Fig. 3, lane 6). This demonstrates that mutant 2D3 is defective in replication. A similar assay on P2 plants was used to demonstrate that mutant 1D3 is also defective in replication. The P2 plants support replication of RNAs 1 and 3 when inoculated with wt 35S/cDNAs 1, 3, and 4 (17) (Fig. 3, lane 7). When the 35S/cDNA 1 in this inoculum was replaced by mutant 1D3, no RNA accumulation was observed (Fig. 3, lane 8).

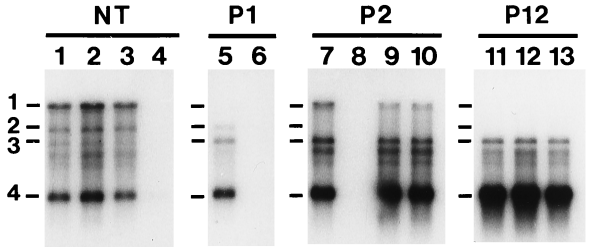

FIG. 3. Accumulation of AMV mutants in tobacco plants inoculated with viral cDNA constructs. In lanes 1 to 4, nontransgenic tobacco plants were used. Inocula consisted of DNAs 1WT, 2WT, and 3WT (lane 1), DNAs 1WT, 2D1, and 3D1 (lane 2), DNAs 1D2, 2WT, and 3D2 (lane 3), or DNAs 1D3, 2D3, and 3WT (lane 4). In lanes 5 and 6, tobacco plants expressing the viral P1 protein were used; they were inoculated with DNAs 2WT, 3WT, and 35S/cDNA4 (4WT) (lane 5) or with DNAs 2D3, 3WT, and 4WT (lane 6). In lanes 7 to 10, plants expressing viral P2 protein were used; they were inoculated with DNAs 1WT, 3WT, plus 4WT (lane 7), DNAs 1D3, 3WT, and 4WT (lane 8), DNAs 1UGD3, 3WT, and 4WT (lane 9), or DNAs 1UG, 3WT, and 4WT (lane 10). In lanes 11 to 13, the results from P12 plants (which express both P1 and P2) are shown. Inocula contained DNA 3WT (lane 11), 3D1 (lane 12), or 3D2 (lane 13). The positions of RNAs 1 to 4 are indicated in the left margin. Abbreviations are explained in the text.

Role of hairpin E in RNA accumulation. The observation that 35S/cDNA mixtures 1WT-2D1-3D1 and 1D2-2WT-3D2 induced wt levels of RNA accumulation in nontransgenic tobacco showed that the mutants in these mixtures were replication competent. In mutants 3D1 and 3D2, the two bottom base pairs of the putative hairpin E are replaced by U-G base pairs. The biological activity of these mutants was further confirmed by inoculation of transgenic tobacco transformed with both the P1 and P2 genes (P12 plants). P12 plants support the replication of RNA 3 when inoculated with wt 35S/cDNA 3 (17) (Fig. 3, lane 11). When the P12 plants were inoculated with mutant 3D1 (Fig. 3, lane 12) or 3D2 (Fig. 3, lane 13), the mutant accumulated at wt levels. If the putative hairpin E plays a role in RNA accumulation, U-G base pairs at its base are apparently tolerated in the chimeric RNAs. To see if U-G base pairs at this position would affect the accumulation of a nonchimeric RNA, the two base pairs at the bottom of hairpin E in RNA 1 were changed into U-G base pairs in mutant 1UG (Fig. 2). When P2 plants were inoculated with a mixture of mutant 1UG and wt 35S/cDNAs 3 and 4, the mutant accumulated at wt levels (Fig. 3, lane 10).

The defect in the accumulation of mutants 1D3 and 2D3 could be due to the presence of two A-C mismatches at the bottom of hairpin E in these mutants. To test this possibility, these mismatches were changed into a G-C and an A-U base pair in mutant 1UGD3 (Fig. 2). When P2 plants were inoculated with a mixture of mutant 1UGD3 and wt 35S/cDNAs 3 and 4, the mutant accumulated at wt levels (Fig. 3, lane 9). This indicates that the predicted structure of hairpin E is correct and that this hairpin is essential to the accumulation of RNAs 1, 2, and 3. Moreover, the results demonstrate that the common 3′-terminal sequences of the three RNAs are functionally equivalent and can be exchanged as long as the secondary structure of hairpin E is not affected.

Deletion analysis of RNA 1 and 2 sequences recognized by the AMV RdRp in vitro. T7 RNA polymerase transcripts of AMV cDNAs 1 and 2 with nonviral G residues at their 5′ ends showed a very low level of infectivity in plants or protoplasts when mixed with RNA 3 (34) but appeared to be active templates for the purified AMV RdRp in an in vitro assay. To map the sequences recognized by the RdRp in RNAs 1 and 2, the deletion mutants shown in Fig. 4 were constructed. The labeled minus-strand RNA products synthesized in vitro by the RdRp

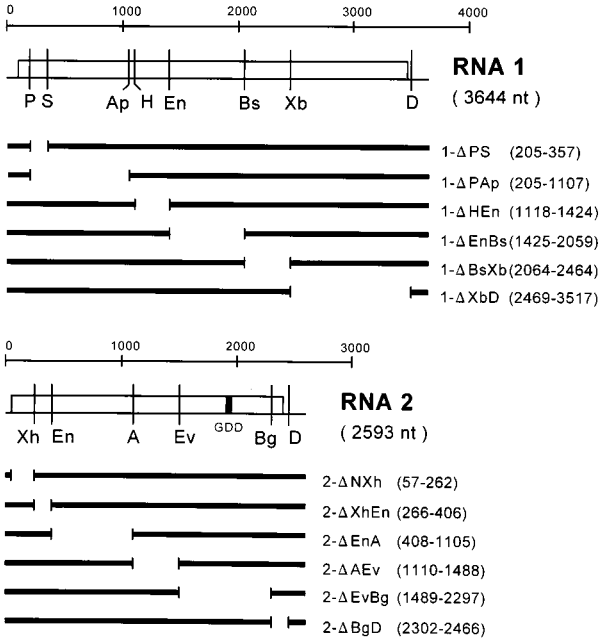

FIG. 4. Schematic drawing of deletion mutants of RNA 1 and RNA 2, which were used as templates for minus-strand RNA synthesis by the AMV RdRp. Deletions (Δ) were made in cDNA copies of AMV RNAs 1 and 2, cloned behind the T7 promoter. The names of the mutants refer to the restriction sites used: P = *Pst*I, S = *Sal*I, Ap = *Apa*LI, H = *Hpa*I, Bs = *Bsp*EI, Xb = *Xba*I, D = *Dra*III, N = *Nco*I, Xh = *Xho*I, En = *Eco*NI, A = *Age*I, Ev = *Eco*RV, and Bg = *Bgl*II. Deleted nucleotides are indicated by the numbers in parentheses. The position of the GDD motif in the P2 open reading frame is indicated.

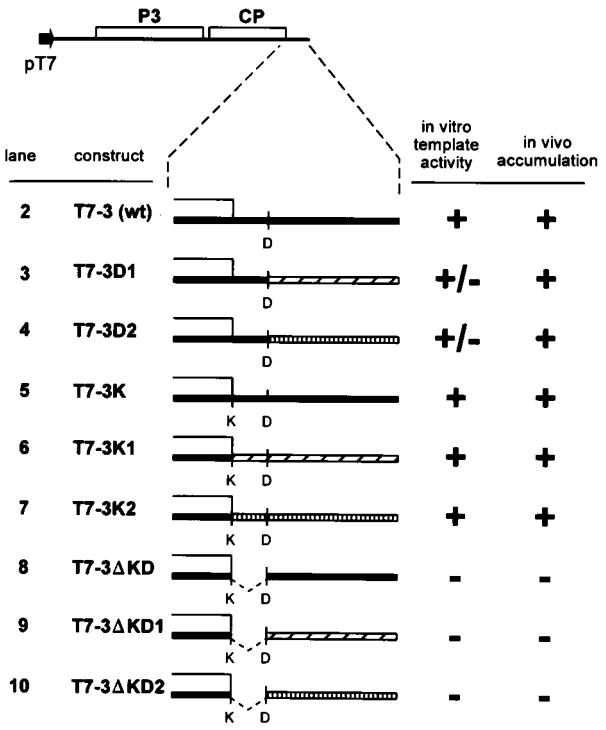

FIG. 6. Schematic representation of hybrid molecules derived from a transcription clone of AMV RNA 3. In mutants T7-3D1 and T7-3D2, the sequence downstream of the *Dra*III restriction site was replaced with the equivalent part of cDNA 1 or cDNA 2, respectively. Mutant T7-3K contains a *Kpn*I restriction site just behind the CP open reading frame. In mutants T7-K1 and T7-K2, the whole 3′ noncoding region was replaced by that of cDNA 1 or cDNA 2, respectively. Mutants T7-KD, T7-KD1, and T7-KD2 were derived from the latter three mutants by deletion of the *Kpn*I-*Dra*III restriction fragment. The numbers on the left refer to the lane numbers in Fig. 7. The table on the right summarizes the results as seen in Fig. 7, where + indicates levels at 100% of wt, +/− corresponds to levels of about 30% of wt, and − indicates that no synthesis or accumulation of RNA was observed.

on RNA 1- and 2-derived templates are shown in Fig. 5A and B, respectively. In the absence of an added template, no RdRp activity is observed (Fig. 5, lanes 1). The wt RNA 1 and RNA 2 transcripts are copied by the RdRp into full-length minus-strand products (Fig. 5, lanes 2). Deletion of sequences between nt 205 (*Pst*I) and nt 2464 (*Xba*I) in RNA 1 had little or no effect on template activity of the RNA in the RdRp assay

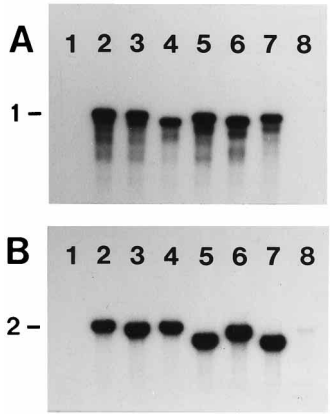

FIG. 5. Autoradiogram of radiolabeled products of minus-strand RNA synthesis by AMV RdRp on in vitro-synthesized derivatives of AMV RNA 1 (A) or RNA 2 (B). (A) Lanes: 1, no added template RNA; 2, full-length RNA 1 transcript; 3, 1-ΔPS; 4, 1-ΔPAp; 5, 1-ΔHEn; 6, 1-ΔEnBs; 7, 1-ΔBsXb; 8, 1-ΔXbD. The position of RNA 1 is indicated in the left margin. (B) Lanes: 1, no added template RNA; 2, full-length RNA 2 transcript; 3, 2-ΔNXh; 4, 2-ΔXhEn; 5, 2-ΔEnA; 6, 2-ΔAEv; 7, 2-ΔEvBg; 8, 2-ΔBgD. The position of RNA2 is indicated in the left margin.

(Fig. 5A, lanes 3 to 7), but deletion of nt 2469 to 3517 in mutant 1-ΔXbD abolished template activity (Fig. 5A, lane 8). This demonstrates that the 3′-terminal 127-nt sequence downstream of the *Dra*III site at position 3517 of RNA 1 is not sufficient for recognition of the RNA by the RdRp. Similarly, deletion analysis of RNA 2 showed that the 3′-terminal 127 nt of this RNA are not sufficient for recognition by the RdRp in vitro. Deletions in RNA 2 from nt 54 (*Nco*I) to nt 2297 (*Bgl*II) did not affect template activity (Fig. 5B, lanes 3 to 7), whereas deletion of the *Bgl*II-*Dra*III fragment (nucleotides 2302 to 2466, mutant 2-ΔBgD) abolished template activity.

Functional equivalence of 3′ UTRs of RNAs 1, 2, and 3 in RNA synthesis in vitro and in vivo. To permit exchange of the full-length 3′ UTRs, *Kpn*I restriction sites were engineered immediately downstream of the UGA stop codons of the P1, P2, and CP genes in AMV cDNAs 1, 2, and 3, respectively. The cDNA 3 clone used was pAL3, which contains a precise fusion of the cDNA to the T7 promoter (16). T7 RNA polymerase transcripts of this clone are infectious to P12 protoplasts and can be used as templates in the in vitro RdRp assay. The wt cDNA 3 clone and the derivative with the *Kpn*I site downstream of the CP gene are designated T7-3 (wt) and T7-3K, respectively, in Fig. 6. These clones were used to make the other constructs shown in Fig. 6. Minus-strand RNA products synthesized in vitro by the AMV RdRp on T7 RNA polymerase transcripts of these constructs are shown in Fig. 7A; Fig. 7B

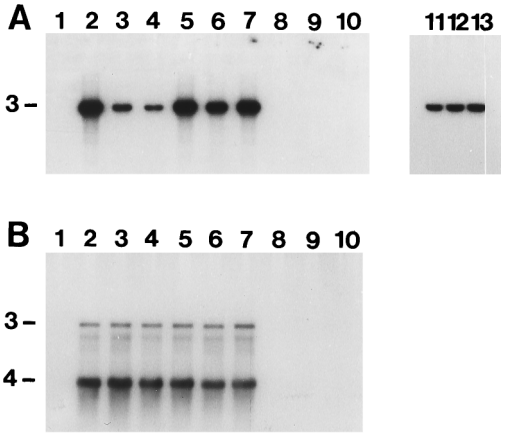

FIG. 7. (A) Autoradiogram of radiolabeled products of in vitro minus-strand RNA synthesis by the AMV RdRp on in vitro-synthesized RNA 3 mutants. Lane 1, no added template; lanes 2 to 10, as indicated in Fig. 6. Lanes 11 to 13 show the results of a separate experiment using the following templates: lane 11, T7-3UG; lane 12, T7-3D1; and lane 13, T7-3D2. The position of RNA 3 is indicated in the left margin. (B) Northern blot showing the accumulation of viral RNAs in P12 plants inoculated with in vitro-synthesized RNA 3 mutants. Lane 1, mock inoculation; lanes 2 to 10, as indicated in Fig. 6. The blot was hybridized with a probe detecting RNA 3 and RNA 4. The positions of these RNAs are indicated in the left margin.

shows the results of a Northern blot analysis of viral RNA accumulation in P12 protoplasts inoculated with these transcripts. The template activity in vitro and replication in vivo of the wt RNA 3 transcript are shown in lanes 2 of Fig. 7A and B, respectively. When the sequence downstream of the *Dra*III site in T7-3 (wt) was replaced by the corresponding sequences of cDNAs 1 and 2 in clones T7-3D1 and T7-3D2, respectively, the in vitro template activity of the transcripts was reduced severalfold (Fig. 7A, lanes 3 and 4). This reduction is probably due to the two U-G base pairs at the bottom of hairpin E in these chimeric RNAs. When the 2 bp present at this position in wt RNA 3 were changed into U-G base pairs to give mutant 3UG (Fig. 2), a similar reduction in template activity was observed (Fig. 7A, lane 11). However, the reduced activity of T7-3D1 and T7-3D2 in vitro did not affect accumulation of the chimeric RNAs in vivo (Fig. 7B, lanes 3 and 4). Introduction of the *Kpn*I site in cDNA 3 resulted in mutation of two nucleotides downstream of the stop codon (in italics) of the CP gene (*UGA*U UUACC to *UGA*GGUACC), but these mutations did not affect the template activity in vitro or infectivity in vivo of the RNA (Fig. 7, lanes 5). Replacement of the sequence downstream of the *Kpn*I site in T7-3K by the full-length 3′ UTRs of cDNAs 1 and 2 in clones T7-3K1 and T7-3K2, respectively, yielded chimeric transcripts with template activity in vitro and infectivity in vivo (Fig. 7, lanes 6 and 7) similar to that of wt RNA 3 (Fig. 7, lanes 2). Deletion of the sequence between the *Kpn*I and *Dra*III sites in T7-3K, T7-3K1, and T7-3K2 yielded mutants T7-3ΔKD, T7-3ΔKD1, and T7-3ΔKD2, respectively (Fig. 6). Transcripts of these deletion mutants showed no template activity in the in vitro RdRp assay and were not infectious to P12 plants (Fig. 7, lanes 8 to 10). This demonstrates that the sequence of the 3′-terminal 127 nt of either AMV RNA 1, 2, or 3 is insufficient for recognition of the viral RNAs by the RdRp in vitro or in vivo.

DISCUSSION

For the replication of a plus-strand RNA virus, the viral RdRp (or components thereof) has to interact with 3′-terminal sequences in the viral RNA. These sequences have been analyzed in the greatest detail for plant viruses ending in a TLS. In addition to being recognized by the viral RdRp, such as TLS is recognized by host proteins that normally interact with tRNAs (4). Here, we analyzed *cis*-acting sequences in the 3′ UTRs of AMV. In the case of this virus, the 3′ termini of the RNAs are recognized by both the viral RdRp and CP (12). By band shift assays, the 3′ UTR of AMV RNA 3 was shown to contain two independent CP binding sites, one located upstream of nucleotide 127 from the 3′ end and one found downstream of this position (20). A CP binding site in the 3′-terminal 39 nt of RNA 3 has been characterized in further detail (8, 21). CPs of AMV and ilarviruses can be exchanged in the process of genome activation (12). In parallel, ilarvirus RNAs sequenced so far end with hairpin structures flanked by AUGC motifs, like the AMV RNAs (21). Although partial sequence data are available for a number of ilarviruses, only for citrus leaf rugose virus has the complete genome been sequenced (7, 23, 24). In the case of citrus leaf rugose virus, all viral RNAs have a 3′ homologous region of 190 nt with putative motifs for CP binding at the 3′ end. However, apart from the CP binding motifs, this 190-nt sequence bears no obvious resemblance to 3′-terminal sequences of RNAs of other ilarviruses or AMV. Our unpublished results show that tobacco streak ilarvirus RNA 4 was not recognized as a template by the AMV RdRp in vitro. These observations might be explained by assuming that the 3′ termini of AMV and ilarvirus RNAs contain common binding sites for CP and unique sequences recognized only by the homologous RdRp.

By using an AMV RdRp preparation from bean leaves, it was shown previously that the 3′-terminal 163 nt of AMV RNA 3 are efficiently recognized in vitro whereas a fragment of 120 nt at the 3′ end was not sufficient for recognition (28). Our present data show that the 3′-terminal 127 nt from RNAs 1, 2, and 3 are insufficient for recognition by the RdRp in vitro. The similarity in template activities of wt RNA 3 and mutants T7-3K1 and T7-3K2 (Fig. 7, lanes 2, 6, and 7) demonstrates that the 3′ UTRs of RNAs 1, 2, and 3 are recognized with similar efficiencies by the RdRp in vitro. Together with the template activities of the deletion mutants of RNAs 1 and 2 shown in Fig. 5, the data indicate that sequences recognized by the RdRp in vitro in plus-strand AMV RNAs 1, 2, and 3 are confined to the 3′ UTRs. Recently, evidence was presented indicating that the P1, P2, and CP genes play a *cis*-acting role in the replication of RNAs 1, 2, and 3, respectively (32, 35). Our results indicate that minus-strand RNA synthesis in vitro does not require *cis*-acting sequences at internal positions of the AMV plus-strand RNAs, as has been reported for bacteriophage Qβ RNA (14).

Inoculation of P12 plants with mutants T7-3ΔKD, T7-3ΔKD1, and T7-3ΔKD2 confirmed that the 3′-terminal region of 127 nt of RNAs 1, 2, and 3 is not sufficient for RNA replication in vivo (Fig. 7B, lanes 8 to 10). Recently, it was shown that deletion of the sequence between the stop codon of the CP gene and nucleotide 165 from the 3′ end of RNA 3 had no effect on RNA 3 replication in vivo (31). Currently, we are analyzing the requirement for RNA replication of the common sequence of 145 nt and unique upstream sequences in the 3′ UTRs of RNAs 1, 2, and 3.

In AMV-infected tobacco plants, the ratio of accumulation of RNAs 1, 2, and 3 is characteristic for a given isolate. Exchanges of the common 3′-terminal sequences of 145 nt (Fig. 3) had little effect on the relative accumulation of the viral RNAs. Similarly, exchanges of the full-length 3′ UTR did not affect the relative accumulation of RNAs 3 and 4 (Fig. 7). Thus, the 22 base substitutions that occur in the 145-nt sequence probably do not regulate the ratio at which the AMV

RNAs accumulate. This may be regulated by *cis*-acting elements involved in initiation of plus-strand RNA synthesis on minus-strand AMV template RNAs. The observation that many of the 22 base substitutions reflect covariation in the stems of hairpins A to E indicates an important role of these hairpins in the life cycle of the virus. Our mutational analysis of hairpin E supports the notion that this stem-loop structure is essential for RNA replication in vivo.

In contrast to the base substitutions in the common 3′-terminal sequence of AMV RNAs, base substitutions in the 3′-terminal TLS of the bromovirus brome mosaic virus (BMV) do affect the ratio at which the three genomic RNAs accumulate (3). In addition to exchanges of TLSs between genomic RNAs of one virus, these structures have also been exchanged between viruses of different genera. In vivo, the BMV RdRp recognized the 3′-terminal sequence of the cucumovirus cucumber mosaic virus when present at the 3′ end of BMV RNA 3. In contrast, a hybrid BMV RNA 2 containing this 3′-terminal sequence from cucumber mosaic virus did not accumulate in tobacco protoplasts or plants (19). Furthermore, BMV RNAs containing the TLS of the tobamovirus tobacco mosaic virus (TMV) were not amplified in vivo, whereas the accumulation of a hybrid TMV RNA containing the BMV TLS showed that this construct was recognized by the TMV RdRp (11). Also, the RdRp of TMV strain L recognized the TLSs of other tobamoviruses (10). In the RNA of the tymovirus turnip yellow mosaic virus, the 3′ TLS could be replaced by those of related tymoviruses without loss of replication, but not by the TLS from BMV or TMV (25).

Swapping experiments have been done not only with plant viruses with 3′-terminal CP binding sites or TLSs but also with 3′-terminal sequences of a plant virus with polyadenylated RNAs. The two genomic RNAs (B-RNA and M-RNA) of the comovirus cowpea mosaic virus (CPMV) contain a homologous 3′-terminal sequence of 65 nt preceeding the poly(A) tail. This sequence can be folded in a Y-shaped structure followed by a U-A-rich hairpin, both of which are important for CPMV RNA replication (5, 22). When the 3′ UTR of CPMV M-RNA was replaced by the 3′ UTR of B-RNA, the chimeric RNA coreplicated efficiently with B-RNA in cowpea protoplasts (27).

Although the 3′ UTRs of AMV RNAs 1, 2, and 3 appear to be functionally equivalent and can be exchanged without loss of replication, our recent experiments indicate that no such exchanges of 5′ UTRs or even longer 5′ sequences of AMV RNAs are possible (33). This indicates that initiation of plus-strand RNA synthesis and that of minus-strand RNA synthesis are basically different processes.

REFERENCES

1. **Bol, J. F., L. van Vloten-Doting, and E. M. J. Jaspars.** 1971. A functional equivalence of top component a RNA and coat protein in the initiation of infection by alfalfa mosaic virus. Virology **46:**73–85.
2. **de Graaff, M., M. R. Man in 't Veld, and E. M. J. Jaspars.** 1995. In vitro evidence that the coat protein of alfalfa mosaic virus plays a direct role in the regulation of plus and minus RNA synthesis: implications for the life cycle of alfalfa mosaic virus. Virology **208:**583–589.
3. **Duggal, R., A. L. N. Rao, and T. C. Hall.** 1992. Unique nucleotide differences in the conserved 3′ termini of brome mosaic virus RNAs are maintained through their optimization of genome replication. Virology **187:**261–270.
4. **Duggal, R., F. C. Lahser, and T. C. Hall.** 1994. *cis*-acting sequences in the replication of plant viruses with plus-sense RNA genomes. Annu. Rev. Phytopathol. **32:**287–309.
5. **Eggen, R., J. Verver, J. Wellink, K. Pleij, A. van Kammen, and R. Goldbach.** 1989. Analysis of sequences involved in cowpea mosaic virus RNA replication using site-specific mutants. Virology **173:**456–464.
6. **Feinberg, A. P., and B. Vogelstein.** 1984. A technique for radiolabeling DNA restriction endonuclease fragments to high specific activity. Anal. Biochem. **137:**266–267.
7. **Ge, X., and S. W. Scott.** 1994. The nucleotide sequence of citrus leaf rugose ilarvirus RNA-2. J. Gen. Virol. **75:**2841–2846.
8. **Houser-Scott, F., M. L. Baer, K. F. Liem, Jr., J. M. Cai, and L. Gehrke.** 1994. Nucleotide sequence and structural determinants of specific binding of coat protein or coat protein peptides to the 3′ untranslated region of alfalfa mosaic virus RNA 4. J. Virol. **68:**2194–2205.
9. **Houwing, C. J., and E. M. J. Jaspars.** 1986. Coat protein blocks the in vitro transcription of the virion RNAs of alfalfa mosaic virus. FEBS Lett. **209:** 284–288.
10. **Ishikawa, M., T. Meshi, Y. Watanabe, and Y. Okada.** 1988. Replication of chimeric tobacco mosaic viruses which carry heterologous combinations of replicase genes and 3′ noncoding regions. Virology **164:**290–293.
11. **Ishikawa, M., P. Kroner, P. Ahlquist, and T. Meshi.** 1991. Biological activities of hybrid RNAs generated by 3′-end exchanges between tobacco mosaic and brome mosaic viruses. J. Virol. **65:**3451–3459.
12. **Jaspars, E. M. J.** 1985. Interaction of alfalfa mosaic virus nucleic acid and protein, p. 155–221. *In* J. W. Davies (ed.), Molecular plant virology. CRC Press, Boca Raton, Fla.
13. **Koper-Zwarthoff, E. C., and J. F. Bol.** 1980. Nucleotide sequence of the putative recognition site for coat protein in the RNAs of alfalfa mosaic virus and tobacco streak virus. Nucleic Acids Res. **8:**3307–3318.
14. **Meyer, F., H. Weber, and C. Weissmann.** 1981. Interactions of Qβ replicase with Qβ RNA. J. Mol. Biol. **153:**631–660.
15. **Murphy, F. A., C. M. Fauquet, D. H. L. Bishop, S. A. Ghabrial, A. W. Jarvis, G. P. Martelli, M. A. Mayo, and M. D. Summers (ed.).** 1995. Virus taxonomy. Sixth report of the International Committee on Taxonomy of Viruses. Arch. Virol. Suppl. 10.
16. **Neeleman, L., A. C. van der Kuyl, and J. F. Bol.** 1991. Role of alfalfa mosaic virus coat protein gene in symptom formation. Virology **181:**687–693.
17. **Neeleman, L., E. A. G. van der Vossen, and J. F. Bol.** 1993. Infection of tobacco with alfalfa mosaic virus cDNAs sheds light on the early function of the coat protein. Virology **196:**883–887.
18. **Quadt, R., H. J. M. Rosdorff, T. W. Hunt, and E. M. J. Jaspars.** 1991. Analysis of the protein composition of alfalfa mosaic virus RNA-dependent RNA polymerase. Virology **182:**309–315.
19. **Rao, A. L. N., and G. L. Grantham.** 1994. Amplification *in vivo* of brome mosaic virus RNAs bearing 3′ noncoding region from cucumber mosaic virus. Virology **204:**478–481.
20. **Reusken, C. B. E. M., L. Neeleman, and J. F. Bol.** 1994. The 3′-untranslated region of alfalfa mosaic virus RNA 3 contains at least two independent binding sites for viral coat protein. Nucleic Acids Res. **22:**1346–1353.
21. **Reusken, C. B. E. M., and J. F. Bol.** 1996. Structural elements of the 3′-terminal coat protein binding site in alfalfa mosaic virus RNAs. Nucleic Acids Res. **24:**2660–2665.
22. **Rohll, J. B., C. L. Holness, G. P. Lomonossoff, and A. J. Maule.** 1993. 3′-Terminal nucleotide sequences important for the accumulation of cowpea mosaic virus M-RNA. Virology **193:**672–679.
23. **Scott, S. W., and X. Ge.** 1995. The complete nucleotide sequence of RNA 3 of citrus leaf rugose and citrus variegation ilarviruses. J. Gen. Virol. **76:**957–963.
24. **Scott, S. W., and X. Ge.** 1995. The nucleotide sequence of citrus leaf rugose virus RNA 1. J. Gen. Virol. **76:**3233–3238.
25. **Skuzeski, J. M., C. S. Bozarth, and T. W. Dreher.** 1996. The turnip yellow mosaic virus tRNA-like structure cannot be replaced by generic tRNA-like elements or by heterologous 3′ untranslated regions known to enhance mRNA expression and stability. J. Virol. **70:**2107–2115.
26. **Taschner, P. E. M., A. C. van der Kuyl, L. Neeleman, and J. F. Bol.** 1991. Replication of an incomplete alfalfa mosaic virus genome in plants transformed with viral replicase genes. Virology **181:**445–450.
27. **van Bokhoven, H., O. Le Gall, D. Kasteel, J. Verver, J. Wellink, and A. van Kammen.** 1993. *cis*- and *trans*-acting elements in cowpea mosaic virus RNA replication. Virology **195:**377–386.
28. **van der Kuyl, A. C., K. Langereis, C. J. Houwing, E. M. J. Jaspars, and J. F. Bol.** 1990. *cis*-acting elements involved in replication of alfalfa mosaic virus RNAs *in vitro*. Virology **176:**346–354.
29. **van der Kuyl, A. C., L. Neeleman, and J. F. Bol.** 1991. Deletion analysis of *cis*- and *trans*-acting elements involved in replication of alfalfa mosaic virus RNA 3 *in vivo*. Virology **183:**687–694.
30. **van der Kuyl, A. C., L. Neeleman, and J. F. Bol.** 1991. Complementation and recombination between alfalfa mosaic virus RNA 3 mutants in tobacco plants. Virology **183:**731–738.
31. **van der Vossen, E. A. G., L. Neeleman, and J. F. Bol.** 1994. Early and late functions of alfalfa mosaic virus coat protein can be mutated separately. Virology **202:**891–903.
32. **van der Vossen, E. A. G., C. B. E. M. Reusken, and J. F. Bol.** 1996. *cis*-preferential stimulation of alfalfa mosaic virus RNA 3 accumulation by the viral coat protein. Virology **220:**163–170.
33. **van Rossum, C. M. A., L. Neeleman, and J. F. Bol.** Manuscript in preparation.
34. **van Rossum, C. M. A.** Unpublished data.
35. **van Rossum, C. M. A., M. L. Garcia, and J. F. Bol.** 1996. Accumulation of alfalfa mosaic virus RNAs 1 and 2 requires the encoded proteins in *cis*. J. Virol. **70:**5100–5105.